EFFECT OF SOURCE-SINK POSITIONS AND THERMAL RADIATION ON MAGNETO-CONVECTION IN A CAVITY

Bindhu RAMACHANDRAN[*], Sivasankaran SIVANANDAM[/***]**

[*]Department of Mathematics, PSG College of Technology, Coimbatore 641004, India
[**]Department of Mathematics, King Abdulaziz University, Jeddah 21589, Saudi Arabia
[***]Department of Mathematics, Saveetha School of Engineering,
Saveetha Institute of Medical and Technical Sciences (SIMATS), Chennai 602105, India

bindhu.psgtech@gmail.com, sd.siva@yahoo.com

received 05 November 2025, revised 03 February 2026, accepted 15 February 2026

Abstract: The prime goal of the current numerical study is to investigate the effect of heater/cooler locations and thermal radiation on convective flow in the presence of a uniform magnetic field in a square cavity with effective thermal zones located partially on the vertically bounded walls. In this study, the active (source/sink) component is measured as half the length of the cavity wall. The inactive portions of the vertical upright wall and horizontal barriers are enabled as adiabatic and thermally insulated. The numerical examination is conducted in detail utilizing the finite volume method and other schemes. This is accomplished by relocating the heater/cooler to five distinct spots along the vertical borders. It is observed that substantial heat transfer occurs at the middle-middle position of the cavity's partially active walls when the magnetic field and radiation levels rise.

Key words: magneto-convection, source-sink locations, partial heating, thermal radiation, cavity

1. INTRODUCTION

The need for capable, highly energy-efficient models has led to a surge in research on enclosures with partially active thermal walls in recent years [1]. Energy-efficient technologies are becoming essential and have many uses in industrial and environmental activities. Therefore, this industry requirement has drawn a number of scholars to focus more on this field [2]. The partially active thermal walls that are put inside an enclosure significantly alter the behavior of the convective flow inside the enclosure, which influences the heat transfer characteristics. See for more details, Sankar et al. [3], & Bhuvaneswari et al. [4]. It is possible that the flow pattern and temperature distribution are affected by the existence of thermal barriers. In this work, the positions of the source and cold sink and thermal radiation on the magnetic-convection pattern are the main sources of interest.

The partial heating and partial cooling of cavities significantly affect convective flow structure and heat transfer amount. This shape is studied because it better represents real engineering systems than fully heated/cooled walls. This model produces localized thermal gradients, which strongly influence fluid motion [5]. This kind of modeling is regularly used in electronics cooling, thermal system design, flat plate solar collectors, and building cooling or heating [6]. The positions of source-sink on convective flow current and thermal spreading in an inclined porous annulus were explored by Sankar et al. [7]. They obtained that a smaller size of sink/source provides higher thermal dissipation with minimal entropy production. Keerthi Reddy et al. [8] discovered the five different single source-sink and three different dual source-sink arrangements on buoyancy convection of nanofluid in an annular section. They found the middle-middle thermally active location makes maximum heat transport.

Natural convection or buoyancy-driven flow is a process in which energy is transported as bulk fluids. This happens due to the dynamic behavior of the fluid, which results from the density differences within a system, [9]. Transient buoyancy influenced convection in a fluid-filled cavity was studied by Kandasamy et al. [10] in which they found that the Nusselt number values show nonlinear behaviour and it depends on the values of the Grashof number. In the paper by Nithyadevi et al. [11] influence of the density inversion parameter on convection and heat transfer in a cavity is executed. It is notified that the transfer rate enhances up to 80% for the placement of partial walls in middle locations. Sinusoidal heating effects on natural convection within a porous chamber were studied out by Sivasankaran and Bhuvaneswari [12], in which they made observations on the relation between the amplitude ratio and heat transport rate. They also established the significance of non-uniform sinusoidal heating within a cavity.

Magneto-convection is a convection mechanism caused by magnetic forces. The Lorentz force generated by the magnetic effect prevents convection currents from forming during this procedure, see, Sivasankaran et al. [13], Biswas et al. [14], Sharma et al. [15]. This interaction between the electrically conducting fluid and the magnetic field is extremely important in the field of control mechanisms, which are widely utilized in the material manufacturing industry [16]. In the work by Bhuvaneswari et al. [17] the impact on convection due to sinusoidal temperature distributions with the presence of a uniform magnetic field is carried out. The results revealed that on increasing the phase deviation, the heat flux first increases and then starts decreasing. The effects of thermal zones

DOI: 10.65731/ama/2026-0019

and the direction of the magnetic field on hydro-magnetic convection in an enclosure were made by Sivasankaran and Bhuvaneswari [18] in which they studied the impact of thermal wall positions. It was observed that the heat transfer rate gets influenced very much when the positions of thermal walls are changed. Gangawane [19] investigated the magneto-convection in an open chamber with partial heating using the lattice Boltzmann method. Jino and Kumar [20] discovered the effect of a bottom-heated-boundary on the magneto-convection of Cu-H2O nanoliquid in a porous domain. MHD convection and entropy generation of nanoliquid in a chamber with a middle hot object are explored by Boulahia [21]. Mishra et al. [22] discovered the impact of the source and Hall effect on magneto-convection of polar fluid in a cylindrical chamber.

The investigation of MHD thermal properties in a water-based hybrid nanofluid-filled non-Darcian porous wavy enclosure demonstrates the intricate relationship between heat transfer, fluid movement, and magnetic fields in a difficult geometric arrangement. Heat management and energy efficiency can be significantly increased by utilizing the advantages of hybrid nanofluids, wavy enclosures, and regulated magnetic fields. Magneto-convection flow of dissipative fluids is strongly affected by the produced magnetic field and thermal radiation. The fluid's velocity, temperature distribution, stability, and general heat transfer properties are all impacted by these intricate and interwoven effects [23]. Advanced thinking and analysis are performed to study more about thermal buoyancy force, which is the significant factor that alters the friction, velocity profiles, and heat transfer inside the domain. For thermal management systems to be optimized in a variety of engineering applications, a thorough understanding of these effects is necessary.

Thermal radiation is another major phenomenon of heat transfer that occurs through electromagnetic waves [24-25]. Recent research has shown a high level of interest in this domain, and radiation flow is encountered in a variety of industrial and environmental activities [26]. Radiative heat transfer is important in many processes, including chamber heating/cooling, nuclear power plants, and astrophysical fluxes, among others [27]. As a result, many researchers have been drawn to this broad spectrum of applications. Radiative magneto-convection, owing to its countless applications in several fields like ionized aerodynamics, aerospace MHD energy systems, advanced aerospace materials manufacturing, nuclear energy system control, etc., has drawn the attention of several researchers [28]. Conjugate transfer of heat by radiation, conduction, and convection enclosed by a solid wall with inclined square geometry was studied by Nouanegue et al. [29]. They found that the heat flux by natural convection gradually increases as the radiation decreases. Mansour et al. [30] investigated the effect of steady natural convection and radiation due to heat using non-equilibrium model in a wavy enclosure. Results depicted that the average Nusselt number increases on increasing waviness and radiation parameter. Observations by Mahapatra et al. [31] revealed that thermal radiation increases the vertical velocity of the fluid and the internal heat generation decreases the vertical velocity of the fluid within a porous medium. Sekhar et al. [32] discovered the thermal radiation and chemical reaction effects on doubly diffusive MHD flow of the Casson fluid. New studies are carried out to analyze the rate of change of thermal and flow transfer inside an enclosed box under the effect of thermal radiation and convective flow driven by buoyancy force with discrete heating and cooling, [33]. Some research on the interaction of thermal radiation with other effects is also shown in the literature [34-35].

It is clearly understood that no research has been directed to get the influence of thermally active parts and thermal radiation on convective stream in the existence of a magnetic field. This work provides a thorough analysis of the changes that occur in temperature distribution and fluid flow inside an enclosure with partially heated walls that is surrounded by an unvarying magnetic flux and thermal radiation. Specifically, the study is conducted by shifting the partially active walls to five distinct locations on the cavity's vertical side. The derived numerical results are thoroughly explored and shown as graphs.

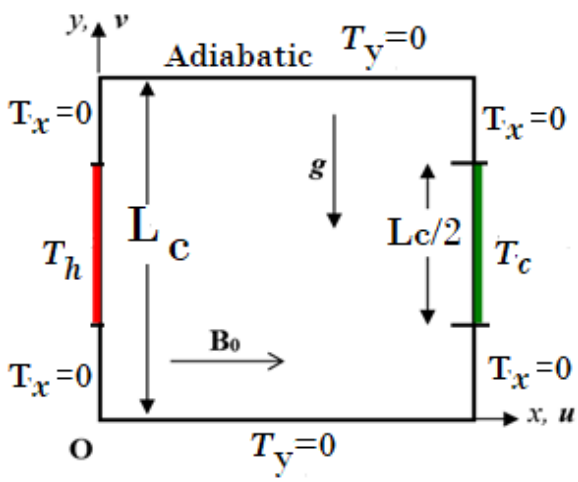

Fig. 1. Physical configuration and boundary conditions

2. MATHEMATICAL MODEL

The model considers a 2-D square cavity of length L_c filled with liquid metal. Its sides are bordered by partially active thermal walls, and its length is half the height of the hollow, as illustrated in Figure 1. The thermal walls are placed in the top-top, middle-middle, bottom-bottom, top-bottom, and bottom-top positions along the surrounded vertical walls, while the upper and lower horizontal walls are left adiabatic. Five different placements of the partial walls are considered here. The placement of both heater and cooler at bottom (top/middle) portion of walls is denoted as BB (TT/MM). Also, placement of heater (cooler) at bottom (top) portion is denoted BT. Its opposite one is denoted as TB. The inactive parts of the side walls, where the heater/cooler are not placed, are considered to be adiabatic. The heater is kept with temperature T_h and it is higher than the cooler temperature T_c. The gravitational force acts in the direction of negative *y*-axis while the uniform magnetic field B_0 acts parallel to the positive *x*-axis. The radiative heat flux is expected to move along both the x and y directions. The following assumptions are taken to examine the model. The flow is laminar and incompressible. The viscous dissipation and the induced magnetic force field are assumed to be minimal, and the formulation is consistent with the Boussinesq approximation for natural convection. The medium is gray and optically thick. The material absorbs and emits radiation uniformly across all wavelengths (gray), and is dense enough that photons undergo multiple scattering/absorption events before escaping (optically thick). Due to the high optical thickness, the radiative transfer equation can be simplified into a diffusion-like process, known as the Rosseland approximation. The radiative heat flux is highly dependent on the local temperature gradient.

Under these physical conditions, the following equations govern the model:

$$\frac{\partial u}{\partial x}+\frac{\partial v}{\partial y}=0 \tag{1}$$

$$\frac{\partial u}{\partial t}+u\frac{\partial u}{\partial x}+v\frac{\partial u}{\partial y}=-\frac{1}{\rho_0}\frac{\partial p}{\partial x}+\upsilon\left[\frac{\partial^2 u}{\partial x^2}+\frac{\partial^2 u}{\partial y^2}\right] \tag{2}$$

$$\frac{\partial v}{\partial t}+u\frac{\partial v}{\partial x}+v\frac{\partial v}{\partial y}=-\frac{1}{\rho_0}\frac{\partial p}{\partial y}+\upsilon\left[\frac{\partial^2 v}{\partial x^2}+\frac{\partial^2 v}{\partial y^2}\right]+g\beta(T-T_0)-\frac{\sigma_e B_0^2 \upsilon}{\rho_0} \tag{3}$$

$$\frac{\partial T}{\partial t}+u\frac{\partial T}{\partial x}+v\frac{\partial T}{\partial y}=\frac{k}{\rho_0 c_p}\left[\frac{\partial^2 T}{\partial x^2}+\frac{\partial^2 T}{\partial y^2}\right]+\frac{1}{\rho_0 c_p}\left[\frac{\partial q_r}{\partial x}+\frac{\partial q_r}{\partial y}\right] \tag{4}$$

Here the variables u and v represent the velocity that acts x and y directions, respectively. The variable T denotes the temperature and p denotes the pressure. The other relevant fluid properties incorporated in the equations are: kinematic viscosity (ν), density(ρ), thermal conductivity (k), electrical conductivity (σ_e)and the coefficient of volumetric expansion (β). The rate of change of heat per unit volume due to radiation along the coordinate axes x and y are given by

$$q_r=\frac{-4\sigma^*}{3K'}\frac{\partial T^4}{\partial x} \quad \text{and} \quad q_r=\frac{-4\sigma^*}{3K'}\frac{\partial T^4}{\partial y} \tag{5}$$

The temperature difference within the flow is assumed to be very small by the Rosseland approximation for radiation. By the use of Taylor series, T^4 is approximated as $T^4 \cong 4{T_0}^3T-3{T_0}^4$, and so, the heat flux due to radiation along the horizontal and vertical direction becomes

$$q_r=\frac{-16\sigma^*{T_o}^3}{3K'}\frac{\partial T}{\partial x} \quad \text{and } q_r=\frac{-16\sigma^*{T_o}^3}{3K'}\frac{\partial T}{\partial y}$$

Therefore, equation (4) reduces to

$$\frac{\partial T}{\partial t}+u\frac{\partial T}{\partial x}+v\frac{\partial T}{\partial y}=\frac{k}{\rho_0 c_p}\left[\frac{\partial^2 T}{\partial x^2}+\frac{\partial^2 T}{\partial y^2}\right]+\frac{1}{\rho_0 c_p}\frac{-16\sigma^*{T_o}^3}{3K'}\left[\frac{\partial^2 T}{\partial x^2}+\frac{\partial^2 T}{\partial y^2}\right] \tag{6}$$

The appropriate initial and boundary conditions are chosen as

$$\begin{aligned}
&t=0: \quad u=v=0; \quad T=0, \quad 0\le x\le L_c, \quad 0\le y\le L_c\\
&t>0: \quad u=v=0; \quad \frac{\partial T}{\partial y}=0, \quad y=0 \text{ and } y=L_c\\
&u=v=0; \quad T=T_h, \text{ at } x=0,\\
&0\le y\le \tfrac{L_c}{2} \quad \text{for bottom heating}\\
&\tfrac{L_c}{4}\le y\le \tfrac{3L_c}{4} \quad \text{for middle heating}\\
&\tfrac{L_c}{2}\le y\le L_c \quad \text{for top heating}\\
&u=v=0; \quad T=T_c, \text{ at } x=L_c\\
&0\le y\le \tfrac{L_c}{2} \quad \text{for bottom cooling}\\
&\tfrac{L_c}{4}\le y\le \tfrac{3L_c}{4} \quad \text{for middle cooling}\\
&\tfrac{L_c}{2}\le y\le L_c \quad \text{for top cooling}\\
&u=v=0; \quad \frac{\partial T}{\partial x}=0, \text{ elsewhere at } x=0 \ \& \ x=L_c.
\end{aligned} \tag{7}$$

Rewriting the above equations in the non-dimensional form by applying the dimensionless variables,

$$X=\frac{x}{L_c},\ Y=\frac{y}{L_c},\ U=\frac{uL_c}{\upsilon},\ V=\frac{vL_c}{\upsilon},\ \tau=\frac{t}{{L_c}^2/\upsilon},$$

$$\theta=\frac{T-T_0}{T_h-T_c},\ P=\frac{p{L_c}^2}{\rho}.$$

Then, we get modified the dimensionless equations as

$$\frac{\partial U}{\partial X}+\frac{\partial V}{\partial Y}=0 \tag{8}$$

$$\frac{\partial U}{\partial \tau}+U\frac{\partial U}{\partial X}+V\frac{\partial V}{\partial Y}+\frac{\partial P}{\partial X}=\frac{\partial^2 U}{\partial X^2}+\frac{\partial^2 U}{\partial Y^2} \tag{9}$$

$$\frac{\partial V}{\partial \tau}+U\frac{\partial V}{\partial X}+V\frac{\partial V}{\partial Y}+\frac{\partial P}{\partial Y}=\frac{\partial^2 V}{\partial X^2}+\frac{\partial^2 V}{\partial Y^2}-Ha^2V+Gr\theta \tag{10}$$

$$\frac{\partial \theta}{\partial \tau}+U\frac{\partial \theta}{\partial X}+V\frac{\partial \theta}{\partial Y}=\left(1+\frac{4}{3}Rd\right)\frac{1}{Pr}\left[\frac{\partial^2 \theta}{\partial X^2}+\frac{\partial^2 \theta}{\partial Y^2}\right] \tag{11}$$

where, $Gr=\frac{g\beta(T_h-T_c){L_c}^3}{\upsilon^2}$ represents the Grashof number, $Ha=B_0L_c\sqrt{\frac{\sigma_e}{\mu}}$ is the Hartmann number, $Pr=\frac{\upsilon}{\alpha}$ denotes the Prandtl number and $Rd=\frac{4\sigma^*{T_0}^3}{kK'}$ is the radiation parameter. Further, the non-dimensionalized initial conditions and boundary conditions are:

$$\begin{aligned}
&\tau=0: \quad U=V=\theta=0; \quad \text{at} \quad 0\le(X,Y)\le 1\\
&\tau>0: \quad U=V=0; \quad \frac{\partial\theta}{\partial Y}=0 \text{ at } Y=0\ \&\ 1\\
&U=V=0;\ \theta=1, \quad \text{at} \quad X=0,\\
&0\le Y\le \tfrac{1}{2} \quad \text{bottom heating}\\
&\tfrac{1}{4}\le Y\le \tfrac{3}{4} \quad \text{middle heating}\\
&\tfrac{1}{2}\le Y\le 1 \quad \text{top heating}\\
&U=V=0;\ \theta=0 \text{ at } X=1,\\
&0\le Y\le \tfrac{1}{2} \quad \text{bottom cooling}\\
&\tfrac{1}{4}\le Y\le \tfrac{3}{4} \quad \text{middle cooling}\\
&\tfrac{1}{2}\le Y\le 1 \quad \text{top cooling}\\
&U=V=0, \quad \frac{\partial\theta}{\partial X}=0 \text{ elsewhere } X=0\ \&\ 1
\end{aligned} \tag{12}$$

The rate of change of heat due to effect of convection and radiation is measured through Nusselt number values and the local measures are measured by the formula:

$$Nu=-\frac{L_c}{k(T_h-T_c)}\left(\frac{\partial T}{\partial x}\right)+\frac{-16\sigma^*{T_o}^3}{3K'}\left(\frac{\partial T}{\partial x}\right) \tag{13}$$

In addition, the average Nusselt number values are estimated using the formula:

$$\overline{Nu}=\frac{2}{L_c}\int_{h_L}^{\frac{L_c}{2}+h_L} Nu\, dY \tag{14}$$

where $h_L=0,\ \frac{L_c}{4},\ \frac{L_c}{2}$ respectively, for bottom, middle and top heating.

3. SOLUTION PROCEDURE

Since the mathematical model consists of system of nonlinear partial differential equations (PDEs), it is hard to find the closed

DOI: 10.65731/ama/2026-0019

form solutions. So, the numerical procedure is proposed here to find the solution of the governing model. The equations from (8) - (11) with boundary conditions (12) are resolved numerically with finite volume method. The convective (diffusive) terms are discretized by QUICK (CDS) schemes. The SIMPLE algorithm is adopted to link the pressure and velocities as described by Versteeg and Malalasekera [36]. The solution domain is divided into finite number of grids. From the grid independent test, it is understand that the grid size 121×121 is enough to get solutions. The resulting sets of simultaneous equations are solved using Gauss Seidel method. The Nusselt number values are obtained by employing trapezoidal rule with a step size of $\Delta x = \frac{1}{120}$ being used. The iterations are carried out until the convergence results are within a tolerance level of 10^{-6}.

Since the comparison is essential task to ensure the accuracy of present calculations, it is proposed a comparison with the existing data from the magneto-convection in an enclosure with fully heated and cooled wall, studied by Rudraiah *et al*. [37]. It is shown in Table 1. The results are agreed well with the present calculation. It gives the confidant on our simulations.

Tab. 1. Comparison of $\overline{Nu}$ with $Pr = 0.733, Rd = 0$

Gr	Ha	$\overline{Nu}$		
		Rudraiah *et al.* [37]	Present	Error (%)
2×10^5	0	4.9198	4.949235	2.94
	10	4.8053	4.871403	6.61
	50	2.8442	2.895173	5.09
	100	1.4317	1.482050	5.04

4. RESULTS AND DISCUSSION

The effects of magneto-convection and thermal radiation inside a cavity bounded with partial walls and moved along the vertical walls of a square cavity is studied for five different locations; particularly, bottom-bottom (BB), bottom-top (BT), middle-middle (MM), top-bottom (TB), and top-top (TT). Other locations such as middle-top, middle-bottom, top-middle and bottom-middle are not discussed, since the effects of heat transfer rate in the former five cases influence more when compared to the latter locations of the thermal walls. To attain a clear insight on the joined effects of radiative heat flux and natural convection with the influence of uniform magnetic field, radiation parameter Rd is varied from 0 to 10. The results thereby obtained are exhibited for three radiation parameter values $Rd = 0, 3, 10$. The values of Hartmann numbers that are chosen for the analysis are 0, 10, 25 and 50.

The streamlines for different locations of the heater/cooler on varying magnetic field and radiation is demonstrated in Figure 2. The investigations are carried out exclusively for the locations bottom-bottom (BB), bottom-top (BT), middle-middle (MM), top-bottom (TB), and top-top (TT). For all the five locations, the presence of heat due to radiation influence the fluid to move in clockwise sense. Also, near the cavity's corners, small eddy formations are observed. Unlike, this scenario, when the radiation is absent, a primary eddy with single nucleus fills the entire cavity for all the thermal locations except for the middle-middle case. While observing the flow pattern of top-bottom partial wall position, a primary eddy with bi-nucleus is observed. These observation infer that when the radiation increases, the formation of eddies near the corners get strengthened.

Figure 3 illustrates the distribution of temperature for different positions of the heater/cooler when the radiation parameter and Hartmann number values are varied. In general, while observing the dissipation of heat, the rate of heat transport is high in the presence of radiation when compared to the absence of radiation. When $Rd = 0$, the isotherms exhibit an early horizontal thermal stratum in the middle of the cavity almost for all locations of the partial walls. From this, it is inferred that convection is the heat exchange mechanism that dominates the distribution of temperature inside the cavity. In contrast, when the radiation parameter value gets increased to 10, it is seen that the isotherms are almost vertical in the middle portion of the cavity and it can be concluded that significant heat exchange in the cavity happens due to radiation. It is vivid that the skewed nature of the thermal stratum significantly depends on the location of heater/cooler. Negligible gradient is observed in the absence of radiation and maximum gradient is seen in the presence of high radiation. Also, when there is no radiation, thin boundary layers formations are observed near the heater for the locations of partial walls at the places bottom-bottom, bottom-top, middle-middle, whereas they are not observed when radiation is present.

In order to obtain the consequence of heat transfer rate for different arrangements of partial walls, discussions are made against Hartmann numbers 0 and 25 and the radiation parameter values being varied from 0 to 10. Figure 4(a-c) and Figure 5(a-c) depict the local Nusselt number values obtained from the analysis for the radiation parameters 0, 3, and 10 when Ha=0 and Ha=25 respectively. The figures are plotted for the height of the cavity versus Nusselt number values obtained. Figure 4(a) illustrates the rate of heat transfer observed when there is no magnetic field and radiation $(Ha = 0, Ra = 0)$. It is seen that, the transfer rate seems to be very high near the edges of the partial wall for the middle-middle arrangement. On the placement of thermal walls at the bottom-bottom and bottom-top, the rate of heat exchange seems to be moderate near the upper edge of the partial wall and on altering the arrangements to top-top and top-bottom positions, a high heat transfer is observed near the lower edge of the thermal wall.

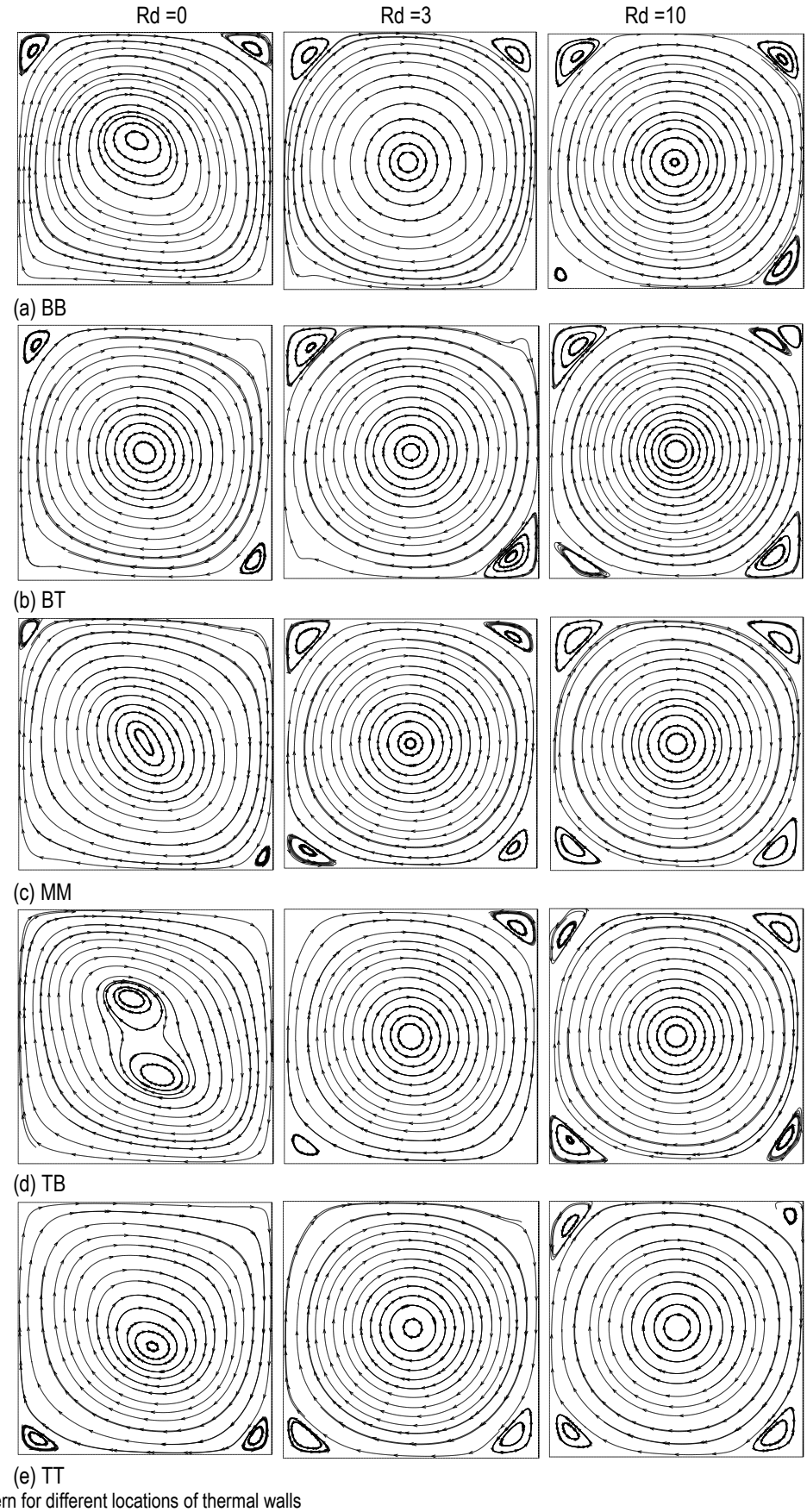

Fig. 2. Streamline pattern for different locations of thermal walls

DOI: 10.65731/ama/2026-0019

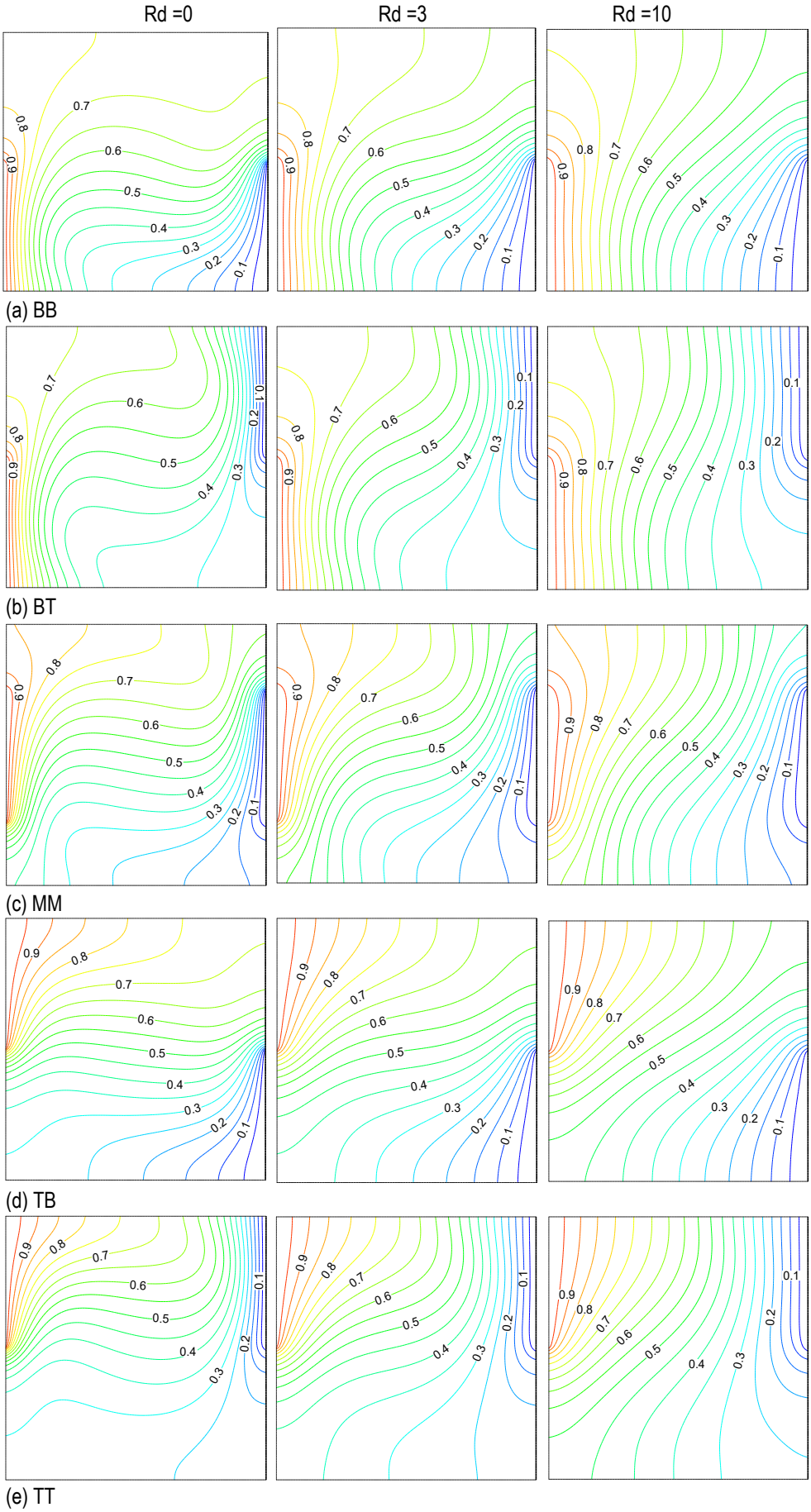

Fig. 3. Isotherms for different locations of partially active thermal walls

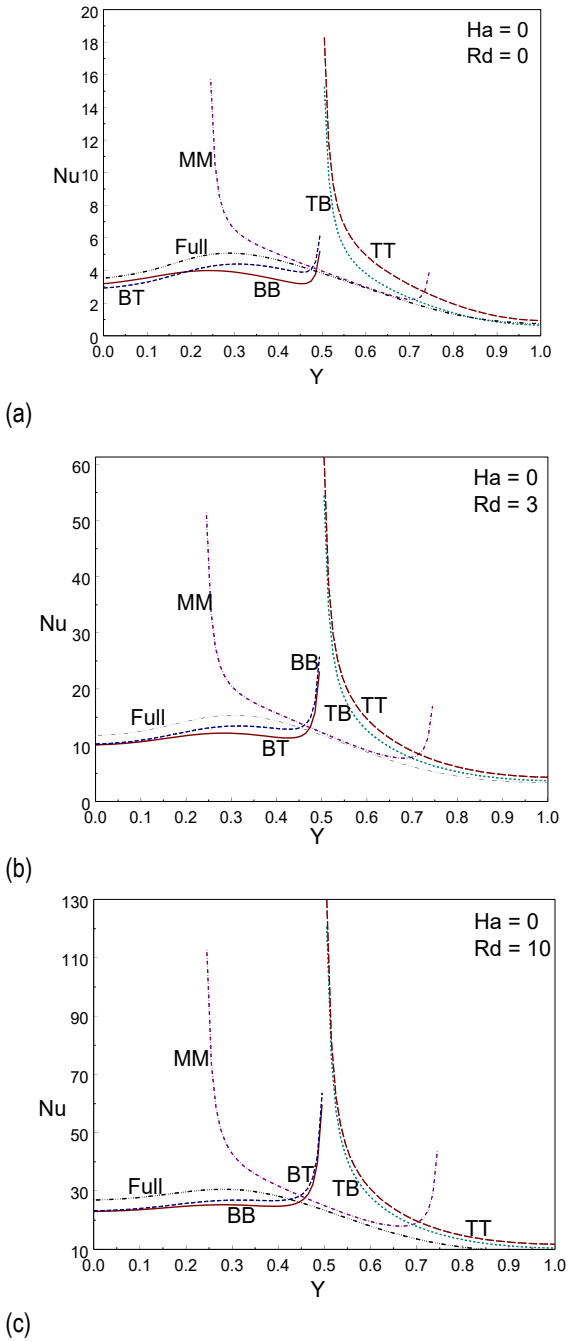

Fig. 4. Local Nusselt number values for different Radiation values when Ha=0

Figure 5(a) exhibits the heat transfer scenario for the presence of magnetic field and no radiation $(Ha = 25,\ Ra = 0)$. Again, it is seen that, enhanced heat transfer is observed when the partially heated walls are kept in middle-middle locations when compared to the other four arrangements of the partially heated thermal walls.For all the arrangements of partial walls and on comparing the effects of partial heating of the cavity when $Rd = 3$ for $Ha = 0$ and $Ha = 25$, thermal transfer rate is seen high for $Ha = 25$. That is, when uniform magnetic field and radiation exist, rate of change of temperature seem to be high. When the radiation parameter value is further increased to 10, again an enhanced heat transfer rate is observed for $Ha = 25$. On comparing all the five different positions of partial walls and for different radiation values, it can be noted that, as the radiation parameter value increases heat transfer rate also increases. Moreover, when the radiation effect exists in the cavity, the magnetic strength applied does not deteriorate the heat flux inside the bounded cavity.

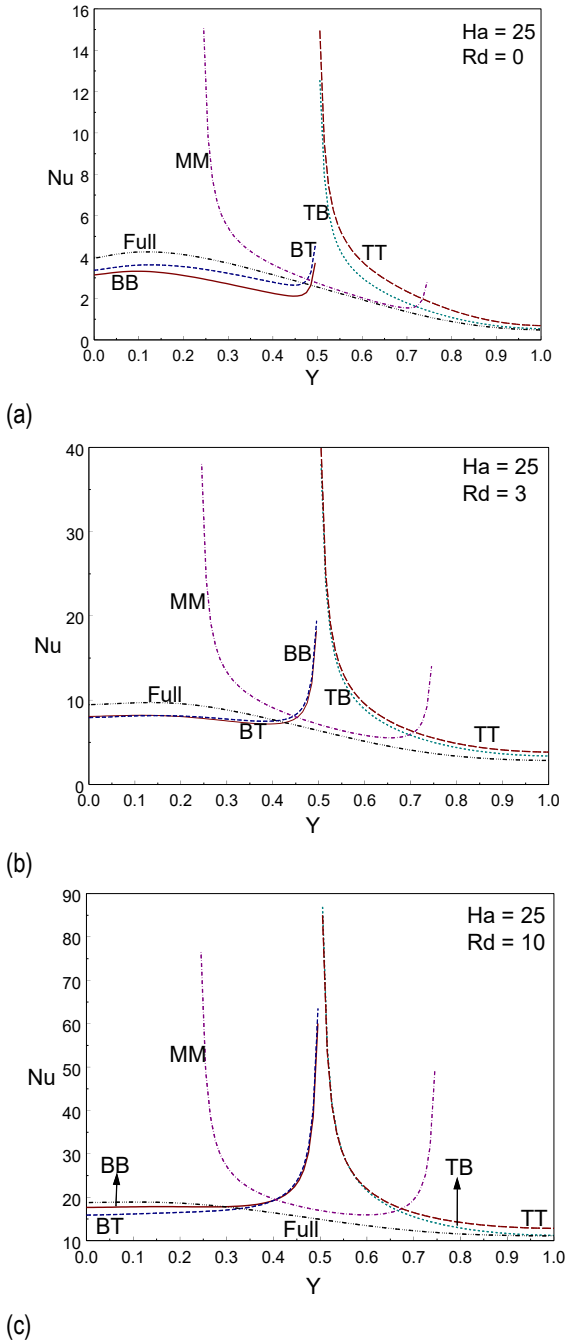

Fig. 5. Local Nusselt number for different Radiation values when Ha=25

Figure 6(a-d) explains the overall heat transfer rate observed from the analysis due to the combined existence of magnetic field and radiation. The figures plotted displays the average Nusselt number values obtained for distinct radiation parameter values. From the results obtained it can be explained that, out of all the five different arrangements of the partially heated walls, the performance of partial heaters in the middle-middle location gives maximum heat transfer whereas the minimum heat exchange is perceived for the location top-bottom. On the other hand, while comparing the performance of walls bounded with partial heaters with that of fully heated ones, partially heated cavity gives enhanced heat exchange rate than the fully heated ones. This rapid and enhanced heat transfer rate in partially heated cavity is

DOI: 10.65731/ama/2026-0019

experienced not only in the absence of magnetic field and radiation, but also in the presence of them. Significantly, it is also noted that, as the magnetic strength increases, the average heat transport rate declines and this is due to the retarding force of magnetic field suppresses the flow speed inside the domain.

Figure 7 shows the heat transfer analysis for different location and various values of Rd. For various values of Rd, the chart shows the incremental heat transfer rate in the presence of radiation compared to the absence of radiation. It is clear that as the radiation parameter intensity increases, so does the average thermal transfer. In the TB position, the magnitude of increment is higher than in other circumstances when Ha=0. That is, the average Nusselt number increases by approximately 96.5%, 258.8%, 404.2%, and 735.7%, respectively, when the Rd value rises from 0 to 1, 3, 5, & 10, for TB case in the absence of a magnetic field. Conversely, for low values of Rd, the level of increment is low at TT case and for greater values of Rd, it is at MM case. When taking Rd values 1,3,5,10, the average Nusselt number at Ha=0 increases by approximately 81.5%, 218.5%, 335.2%, and 580.7%, at the TT case and MM case, respectively. When the Rd value increases from 0 to 1, 3, 5, & 10, respectively, in the presence of a high magnetic field (Ha=50), the average Nusselt number increases by approximately 99.4%, 305.9%, 516.8%, and 1048.8% for the TB case. When Ha=50, that is, 59.1%, 199.9%, 348.8%, and 726.8%, the level of increment is low at the BT scenario. See Fig. 7(c). A similar pattern is noted in instances with mild and moderate magnetic fields.

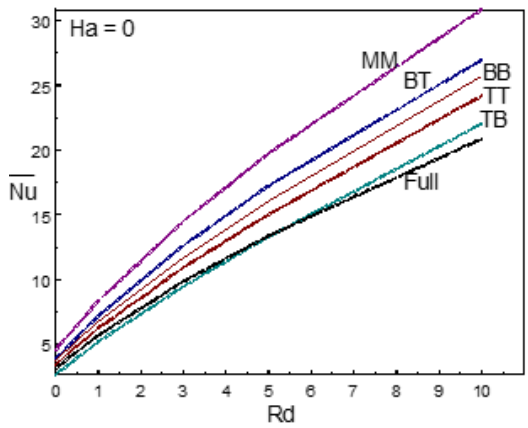

a)

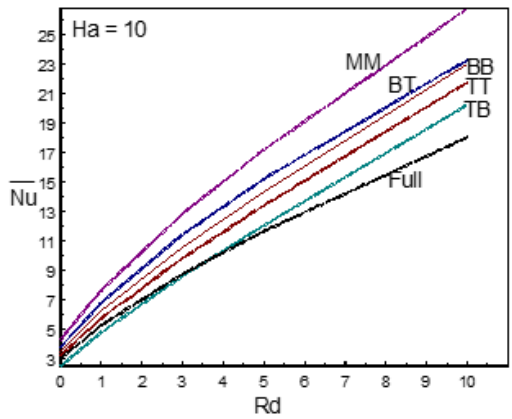

b)

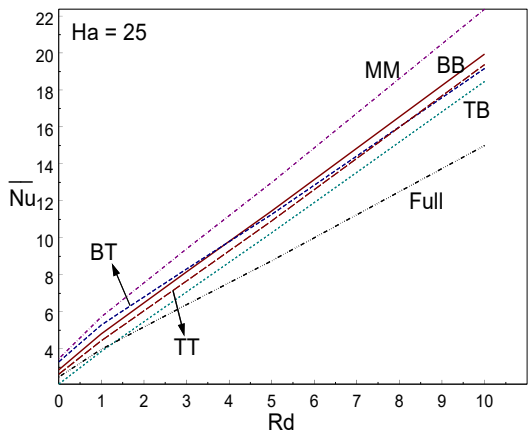

(c)

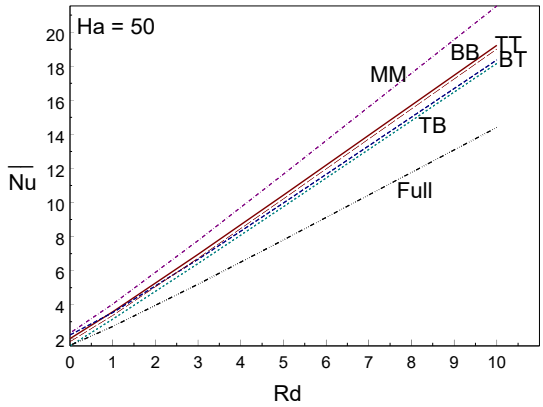

(d)

Fig. 6. Average Nusselt number values for different Hartmann number

Figure 8(a-c) exhibits the influence between partially heated/cooled walls and fully (differentially) heated wall of the enclosed region. The graph gives a clear comparison of the average heat transfer between the fully heated wall and different heater/cooler placements. Based on the comparison, it can be concluded that for all values of Rd and Ha, greater heat transfer occurs when the heater and cooler are positioned in the middle of the wall. However, the TB instance shows the reverse trend, with a lower heat transmission rate than the fully heated or cooled wall. The average heat transfer rate increases by approximately 44.3%, 46.7%, 47.3%, 47.5%, and 48% for Rd = 0, 1, 3, 5, 10, and so on, when the heater/cooler is positioned in the center of the wall(s) without a magnetic field. The average heat transport rate increases by approximately 44.7%, 48.4%, 49.3%, 49.5%, 49.5% for Rd=0,1,3,5,10, respectively, when the heater/cooler is positioned in the middle of the wall(s) at Ha=50. It is known that the thermally inactive/adiabatic region surrounding the heater will facilitate convection and promote efficient thermal mixing. However, when there are walls or barriers near the heater inside the enclosure, it inhibits convective movement and decreases the average heat transfer rate. It is important to note that the cooler should be situated at the same height as or above the heat source to facilitate convection. These results are highly beneficial for the designing of electronic gadgets and equipment, cooling of buildings and thermal systems.

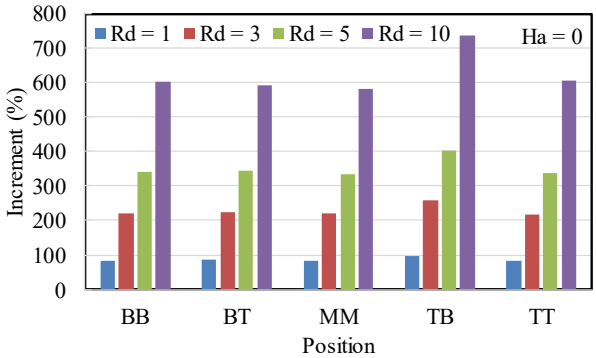

(a)

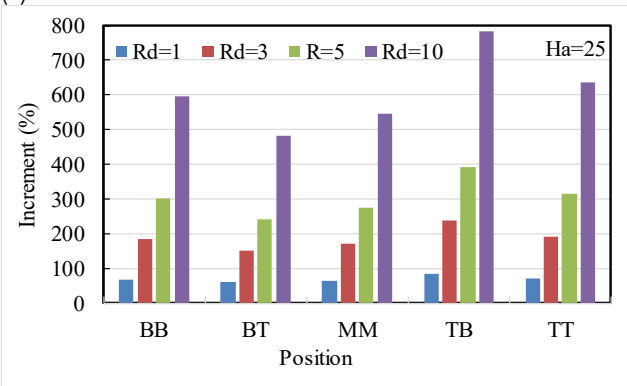

(b)

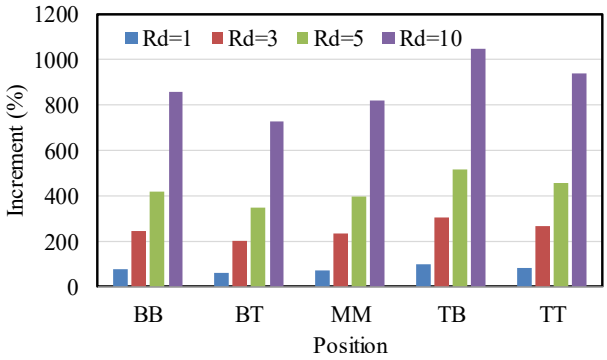

(c)

Fig. 7. Heat transfer increment for different location and Rd

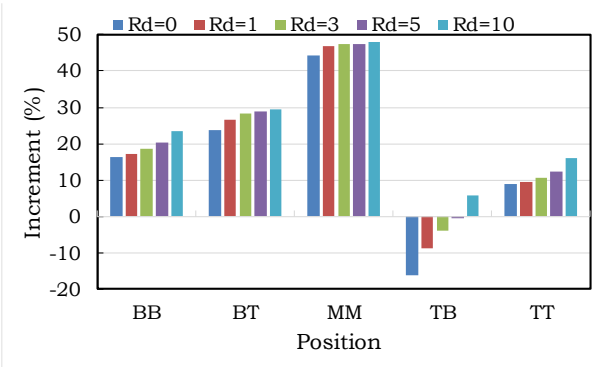

(a)

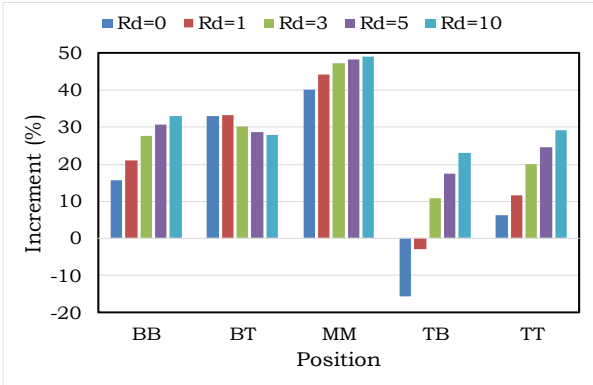

(b)

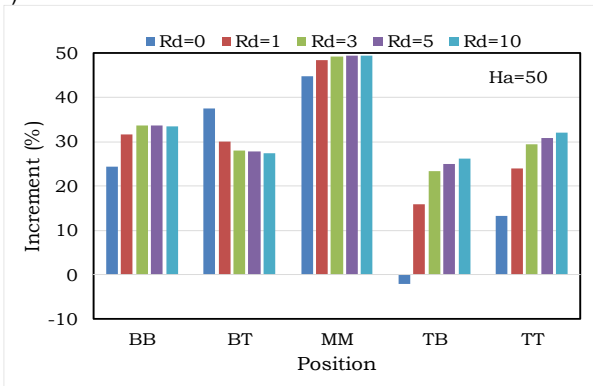

(c)

Fig. 8. Comparison of heat transfer rate for different positions with fully heated wall

5. CONCLUSION

The combined effects of magneto-convection-radiation inside a bounded cavity with partially active thermal boundaries kept in various positions moving along the sidewall are studied and the following results are enumerated below:

- For all five cases, a clockwise circulation filling the majority of the cavity. A primary vortex with a single core is present in all cases except the top-bottom arrangement. Increase in the radiation parameter results in the development of reinforced secondary cells near the corners of the cavity.
- The even spread of isotherms within the cavity indicates convective transport as the dominant mode. The occurrences of thin boundary layers near the heater are noticed in the absence of radiation.
- This enhanced mean heat transfer rate in partially heated cavity is experienced not only in the absence of magnetic field and radiation, but also in the presence of them.
- The average heat transport rate decreases in all heater/cooler locations as the magnetic field strength increases when thermal radiation is present.
- The heat exchange rate is significantly impacted by the specific location of the partial heater/cooler.
- It can be inferred from comparing fully heated and partly active walls that placing the heater/cooler in the middle of the wall results in increased heat transfer for all Rd and Ha values. On the contrary, the TB case displays a reverse pattern, with a reduced heat transmission rate compared to the wall that is fully heated/cooled. This demonstrates that enclosures with partially active walls result in increased heat exchange efficiency.

DOI: 10.65731/ama/2026-0019

REFERENCES

1. Kuhn D, Oosthuizen PH. Unsteady natural convection in a partially heated rectangular cavity. ASME J Heat Mass Transfer. 1987;109:798–801.
2. Bouchmel M, Ferhi M, Abbassi MA. Numerical study of MHD mixed convection of nanofluid flow in a double lid convergent cavity. Acta Mech Autom. 2025;19(2):232–242.
3. Sankar M, Bhuvaneswari M, Sivasankaran S, Do Y. Buoyancy-induced convection in a porous cavity with partially thermally active sidewalls. Int J Heat Mass Transfer. 2011;54:5173–5182.
4. Bhuvaneswari M, Sivasankaran S, Kim YJ. Effect of aspect ratio on convection in a porous enclosure with partially active thermal walls. Comput Math Appl. 2011;62:3844–3856.
5. Sankar M, Park J, Kim D, Do Y. Numerical study of natural convection in a vertical porous annulus with an internal heat source: Effect of discrete heating. Numer Heat Transfer A Appl. 2013;63(9):687–712.
6. Sankar M, Park J, Do Y. Natural convection in a vertical annuli with discrete heat sources. Numer Heat Transfer A Appl. 2011;59(8): 594–615.
7. Sankar M, Kumara Swamy HA, Al-Mdallal Q, Wakif A. Non-Darcy nanoliquid buoyant flow and entropy generation analysis in an inclined porous annulus: Effect of source-sink arrangement. Alex Eng J. 2023;68:239–261.
8. Keerthi Reddy N, Sankar M, Jang B. Impact of thermal source-sink arrangements on buoyant convection in a nanofluid-filled annular enclosure. J Heat Transfer. 2022;144(11):112601.
9. Janaiah C, Saidi Reddy B. Modelling of 3-D Casson–nano–Oldroyd-B fluid flow with Cattaneo–Christov double diffusion effects: Applications in biomedical engineering. Model Earth Syst Environ. 2025;11:412.
10. Kandaswamy P, Sivasankaran S, Nithyadevi N. Buoyancy-driven convection of water near its density maximum with partially active vertical walls. Int J Heat Mass Transfer. 2007;50:942–948.
11. Nithyadevi N, Sivasankaran S, Kandasamy P. Buoyancy-driven convection of water near its density maximum with time periodic partially active vertical walls. Meccanica. 2007;42:503–510.
12. Sivasankaran S, Bhuvaneswari M. Natural convection in a porous cavity with sinusoidal heating on both sidewalls. Numer Heat Transfer A Appl. 2013;63:14–30.
13. Sivasankaran S, Lee J, Bhuvaneswari M. Effect of a partition on hydromagnetic convection in an enclosure. Arab J Sci Eng. 2011;36:1393–1406.
14. Biswas N, Mandal DK, Manna NK, Reddy GRS, Chamkha AJ. Magnetohydrodynamic thermal characteristics of water-based hybrid nanofluid-filled non-Darcian porous wavy enclosure: Effect of undulation. Int J Numer Methods Heat Fluid Flow. 2022;32:1742–1777.
15. Sharma M, Sharma BK, Kumawat C, Jalan AK, Radwan N. Computational analysis of MHD nanofluid flow across a heated square cylinder with heat transfer and entropy generation. Acta Mech Autom. 2024;18(3):536–547.
16. Sudarmozhi K, Iranian D, Ilyas. Chemical reaction effect across the moving flat plate with heat generation and MHD flow of Maxwell fluid with viscous dissipation. Int J Mod Phys B. 2025;39:03.
17. Bhuvaneswari M, Sivasankaran S, Kim YJ. Magnetoconvection in a square enclosure with sinusoidal temperature distributions on both side walls. Numer Heat Transfer A Appl. 2011;59:167–184.
18. Sivasankaran S, Bhuvaneswari M. Effect of thermally active zones and direction of magnetic field on hydromagnetic convection in an enclosure. Therm Sci. 2011;15:367–382.
19. Gangawane KM. MHD free convection in a partially heated open-ended square cavity: Effect of angle of magnetic field and heater location. Int J Appl Comput Math. 2019;5:63.
20. Jino L, Kumar AV. Cu-water nanofluid MHD quadratic natural convection on square porous cavity. Int J Appl Comput Math. 2021;7:164.
21. Boulahia Z. A detailed numerical investigation for various types of entropy generation and magnetohydrodynamic (MHD) free convection within a corrugated cavity comprising nanofluid and a hot object positioned in the middle. Int J Appl Comput Math. 2021;7:213.
22. Mishra M, Panda JP, Sahoo SS. An analytical investigation of MHD natural convective flow of a polar fluid in two vertical concentric cylinders with Hall current and heat source. Int J Appl Comput Math. 2024;10:75.
23. DehghanAfifi M, Jalili B, Mirzaei AM. The effects of thermal radiation, thermal conductivity, and variable viscosity on ferrofluid in porous medium under magnetic field. World J Eng. 2024;ahead-of-print.
24. Karthik S, Iranian D, Ariana A, Alshehery S, Khan I. Significance of thermal radiation on MHD stagnation point flow of Powell–Eyring fluid: A heat and mass transfer problem. J Radiat Res Appl Sci. 2025;18:101383.
25. Sharma PK, Sharma BK, Kumar A. Mathematical analysis of chemically reacting species and radiation effects on MHD free convective flow through a rotating porous medium. Acta Mech Autom. 2024;18(2):193–203.
26. Sun Y, Li X, Zhao J, Yang H. Investigation of transient coupled conduction and radiation heat transfer in the linearly anisotropic scattering cylindrical medium by spectral collocation method. Int J Therm Sci. 2022;172:107308.
27. Kumar B, Seth GS, Nandkeolyar R, Chamkha AJ. Outlining the impact of induced magnetic field and thermal radiation on magnetoconvection flow of dissipative fluid. Int J Therm Sci. 2019;146:106101.
28. Ghalambaz M, Sabour M, Pop I, Wen D. Free convection heat transfer of MgO-MWCNTs/EG hybrid nanofluid in a porous complex shaped cavity with MHD and thermal radiation effects. Int J Numer Methods Heat Fluid Flow. 2019;29:4349–4376.
29. Nouanegue HF, Muftuoglu A, Bilgen E. Heat transfer by natural convection, conduction and radiation in an inclined square enclosure bounded with a solid wall. Int J Therm Sci. 2009;48:871–880.
30. Mansour MA, Abdul-El-Aziz MM, Mohamed RA, Ahmed SE. Numerical simulation of natural convection in wavy porous cavities under the influence of thermal radiation using a thermal non-equilibrium model. Transp Porous Media. 2011;86:585–600.
31. Mahapatra TR, Pal D, Mondal S. Combined effects of thermal radiation and heat generation on natural convection in a square cavity filled with Darcy–Forchheimer porous medium. Int J Appl Comput Math. 2012;4:359–368.
32. Sekhar BC, Kumar PV, Veera Krishna M. Chemical reaction, thermal radiation and Newtonian heating impacts on unsteady MHD rotating Casson fluid flow past an infinite vertical porous surface. Int J Appl Comput Math. 2024;10:157.
33. Sivasankaran S, Bhuvaneswari M, Alzahrani AK. Numerical simulation on convection of non-Newtonian fluid in a porous enclosure with non-uniform heating and thermal radiation. Alex Eng J. 2020;59:3315–3323.
34. Reddy P, Sreedevi P. Thermal radiation impact on heat and mass transfer analysis of nanofluids inside a cavity with gyrotactic microorganisms. Int J Numer Methods Heat Fluid Flow. 2023;33:3839–3865.
35. Sivasankaran S, Bhuvaneswari M, Amer A. Numerical study on buoyant convection and thermal radiation in a cavity with various thermal sources and Cattaneo–Christov heat flux. Case Stud Therm Eng. 2021;27:101207.
36. Versteeg HK, Malalasekera W. An introduction to computational fluid dynamics: The finite volume method. 2nd ed. England: Pearson; 2007.
37. Rudraiah N, Barron RM, Venkatachalappa M, Subbaraya CK. Effect of a magnetic field on free convection in a rectangular enclosure. Int J Eng Sci. 1995;33:1075–1084.

Bindhu Ramachandran: https://orcid.org/0000-0003-1247-9146

Sivasankaran Sivanandam: https://orcid.org/0000-0001-9443-7091

This work is licensed under the Creative Commons BY-NC-ND 4.0 license.